ACS OMEGA

http://pubs.acs.org/journal/acsodf

Article

Poly(3-hydroxybutyrate-*co*-3-hydroxyvalerate) Electrospun Nanofibers Containing Natural Deep Eutectic Solvents Exhibiting a 3D Rugose Morphology and Charge Retention Properties

Ahmet Ozan Basar, Cristina Prieto,* María Pardo-Figuerez, and Jose M. Lagaron*

Cite This: *ACS Omega* 2023, 8, 3798−3811

Read Online

ACCESS | Metrics & More | Article Recommendations

ABSTRACT: In the present study, electrospun nanofibers of poly(3-hydroxybutyrate-*co*-3-hydroxyvalerate) (PHBV), a biodegradable polyester, containing natural deep eutectic solvents (NADES) were obtained and reported for the first time, exhibiting an unreported 3D morphology and enhanced charge retention properties. Choline chloride (ChCl)/urea/water in a molar ratio of 1:2:1 was used as the NADES model system. Electrospun nanofibers were produced from a 10 wt % solution of PHBV containing 26 wt % NADES with respect to the polymer and were deposited on different substrates, that is, aluminum foil and non-woven spunbond polypropylene (PP). The morphology and charge retention ability were characterized under different conditions and on different substrates. The attained fiber morphology for the NADES-containing mats showed an average fiber diameter of around 300 nm, whereas the pure PHBV polymer under the same conditions produced electrospun fibers of around 880 nm. However, the deposition of PHBV/ChCl/urea/water fibers resulted in a surprising macroscopic rugose 3D surface morphology made of aligned nanofibers when processed at 50% relative humidity (RH). The nanofiber grammages above which this 3D morphology, associated with NADES-induced charge retention, formed was found to be dependent on the substrate used and RH. This morphology was not seen at 20% RH nor when pure PHBV was produced. Charge stability studies revealed that PHBV/ChCl/urea/water nanofibers exhibited lasting charge retention, especially when sandwiched between spunbond polypropylene textiles. Finally, such multilayer structures containing a very thin double layer of PHBV/ChCl/urea/water fibers after corona treatment exhibited improved paraffin aerosol penetration, which was ascribed to the combination of thinner fibers and their charge retention capacity. The here-developed electrospun PHBV fibers containing NADES demonstrated for the first time a new potential application as electret filter media.

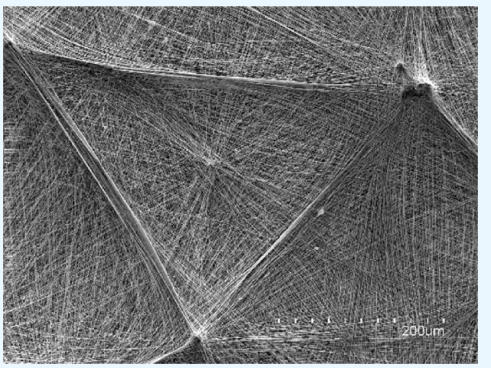

1. INTRODUCTION

Fibrous materials have become advantageous as filter media due to their three-dimensional arrangement of fibers, large surface-to-volume ratio, high porosity, small pore size, and high barrier performance.[1] On top of this, the addition of electrostatic charges to the filter media further improves the filtration efficiency by the electrostatic attraction of fine particulates without increasing the pressure drop.[2] These electrostatically charged fibrous materials, or fibrous electrets, are dielectric materials exhibiting a quasi-permanent external electrostatic field. Electrets contribute to the improvement in the filtration efficiency with a minimum impact on breathing resistance.[3] Thus, such materials are often used as high-performance filters in products such as protective surgical masks and respirators.[1,4]

The filtration mechanism of fibrous electret materials is to a significant extent attributed to the charged fibers attracting the penetrating particles.[5] For this reason, the charge retention capacity and electrostatic charge stability of the filter media are crucial due to their direct link with their high filtration efficiency and reliability.[6,7] The charge retention capacity is generally controlled by the electrical conductivity and the energy level of localized trap sites[8] and may decay over time under environmental conditions such as humidity, wetting, or temperature.[1,8] Hence, it is of paramount importance to continue to develop research into new materials that can be used for this application as filter media.

Spunbond polypropylene (PP) is widely used as a non-woven material in medical masks and respirators due to its ease of processing, much-needed mechanical strength, hydrophobicity, and lower air resistance.[9,10] However, they suffer from poor filtration performance for fine particles when used alone.[11] In many citations relating to protective equipment,

Received: September 8, 2022
Accepted: December 6, 2022
Published: January 20, 2023

one approach to solve this drawback is to use spunbond nonwoven materials as the external mechanical support for the core electrostatic filtration layer, typically made of meltblown polypropylene, that can effectively filter finer particles. The typical N95 respirator is a good example for this, consisting of two or three piles of a dielectric material layer with a quasi-permanent electrical charge (electrostatic filtration layer) between two layers of spunbond polypropylene.[10] However, the polypropylene layers used in respirators are thick petroleum-derived filtration materials, and new alternatives with higher filtration efficiency per grammage are of interest, in that they may potentially improve sustainability by both reducing material consumption and having alternative end-of-life scenarios such as organic recycling when made of biodegradable polymers.[12]

Poly(3-hydroxybutyrate-*co*-3-hydroxyvalerate) (PHBV) is a biobased and biodegradable copolymer composed of the homopolymer poly(3-hydroxybutyrate) (PHB) with hydroxyvalerate (HV) units along the backbone.[13−15] PHBV has become a very versatile polyester with application in different sectors due to, depending on the HV molar content, its balanced physical properties, excellent biocompatibility and biodegradability characteristics, and industrial-scale production.[16−18] In addition, PHBV can be further modified with other agents to improve and expand its industrial relevance and application areas.[19,20]

The use of deep eutectic solvents (DES) is a promising approach to modify the characteristics of PHBV. The term "eutectic" describes a homogeneous mixture of two different solid species, which at a unique molar ratio form a joint superlattice structure with extraordinary properties.[21] DES consist of an eutectic mixture of two (or more) components, namely a hydrogen bond acceptor (HBA), such as quaternary ammonium halide salts and metal chlorides, and a hydrogen bond donor, such as alcohols, amides, and carboxylic acids, which can self-associate to lead to a liquid temperature of their mixture significantly lower than the pure equivalents.[22] Moreover, a kind of DES called natural deep eutectic solvents (NADES) exist, which are solely based on primary metabolites, such as amino acids, organic acids, sugars, or choline derivatives; this also make them fully represent green chemistry principles.[22,23] These new kinds of solvents (DES and NADES) have risen in popularity due to their unique physicochemical properties, such as negligible volatility, an extensive variety of polarity, a liquid state far below 0 °C, high solubilization and stabilization capacity for a broad range of compounds, high extraction performance, and plasticization properties.[22,24,25] Moreover, DES present advantages, such as relatively low cost, biodegradability, biocompatibility, easy production, and nontoxicity, and therefore represent an alternative to organic or other toxic solvents.[26]

In this sense, electrospinning is an innovative technology that can entrap different compounds into polymeric nanofibers.[27] The electrospinning process involves the evaporation of liquid polymeric solutions flowing out of a capillary nozzle due to a high electrical potential, which while flying and stretching toward the collector leads to the generation of dry fibers at room temperature. This technology has revealed a great potential to generate ultrathin fibrous mats made of a wide range of polymeric materials with fiber diameters ranging from a few microns to several nanometers[28] with the capacity to be used in filtering devices with high filtration efficiency.[29] However, the entrapment of DES into nanofibers via the electrospinning technique is a fairly new research area, and there are only a few related studies. For instance, Sousa et al. revealed the electrospinning with DES for the first time, reporting that the electrospinnability of agar was improved with the incorporation of (2-hydroxyethyl)-trimethylammonium chloride and urea at a 1:2 molar ratio.[30] In another study by Mano et al., the electrospinning of poly(vinyl alcohol) (PVA) fibers with encapsulated choline chloride/citric acid (1:1) was carried out, and the authors suggested that the developed system could be promising for drug delivery.[31] In a follow-up study by the same authors, a therapeutic deep-eutectic solvent (THEDES) made of choline chloride/mandelic acid (1:2) was encapsulated in gelatin fibers using the electrospinning technique.[32] More recently in 2020, Khatri et al. successfully electrospun zein nanofibers using DES [choline chloride/furfuryl alcohol (2:1)].[33]

In this seminal paper, NADES-containing PHBV nanofibers with charge retention capacity were reported for the first time with potential interest in, among other areas, air filtration applications. A surprising rugose morphology was attained, and the parameters that affect this were ascertained. In this context, the electrostatic charge stability was explored with surface potential measurements under different relative humidity (RH) conditions and different configurations. Lastly, the air filtration capabilities of NADES-containing PHBV fibers, exhibiting electret behavior, sandwiched between a model spunbond polypropylene substrate were assessed.

2. MATERIALS AND METHODS

2.1. Materials. Commercial PHBV ENMAT Y1000P was purchased from Tianan Biologic Materials (Ningbo, China). According to the manufacturer, the density and the molecular weight (MW) of the biopolymer resins were 1.23 g/cm^3 and ∼2.8 × 10^5 g/mol, respectively, while the molar fraction of HV in the copolymer was 2%. 2,2,2-Trifluoroethanol (TFE) with ≥99% purity was purchased from Merck (Darmstadt, Germany). Choline chloride (ChCl) and urea with purities of ≥98% and ≥99%, respectively, and potassium chloride were purchased from Sigma-Aldrich (St. Louis, MO, USA). As a model substrate, a non-woven spunbond polypropylene material of 17 g/m^2 (PP, NVEVOLUTIA, Valencia, Spain) was used. Distilled water with a conductivity of 2.55 μS/cm was used throughout the study.

2.2. Preparation of NDES. The system ChCl/urea/water was selected as a model NADES. Prior to use, choline chloride was dried at 65 °C under vacuum (Vaciotem-T, JP Selecta, Barcelona, Spain) for 24 h to remove any possible moisture. The system ChCl/urea/water was prepared by weighing and mixing the components in an appropriate molar ratio of 1:2:1. The mixture was then heated under stirring at 80 °C until a clear colorless liquid was obtained. The mixtures remained in the liquid form after cooling to room temperature. Finally, the prepared NADES was stored in a desiccator until further use.

2.3. Electrospinning. PHBV solutions were prepared by dissolving 10 wt % of PHBV in TFE at 50 °C through gentle stirring overnight. Thereafter, ChCl, urea, and water were added in a 1:2:1 ratio to PHBV solutions to attain a final NADES concentration of 26 wt % in PHBV fibers . The resultant mixture was homogenized using a TX4 digital vortex mixer from Velp (Usmate, Italy). Then, the ready-prepared solutions were electrospun using a high-throughput Fluidnatek LE-500 pilot line from Bioinicia S.L. (Valencia, Spain). The equipment was set to lab mode configuration with a single

https://doi.org/10.1021/acsomega.2c05838
ACS Omega 2023, 8, 3798−3811

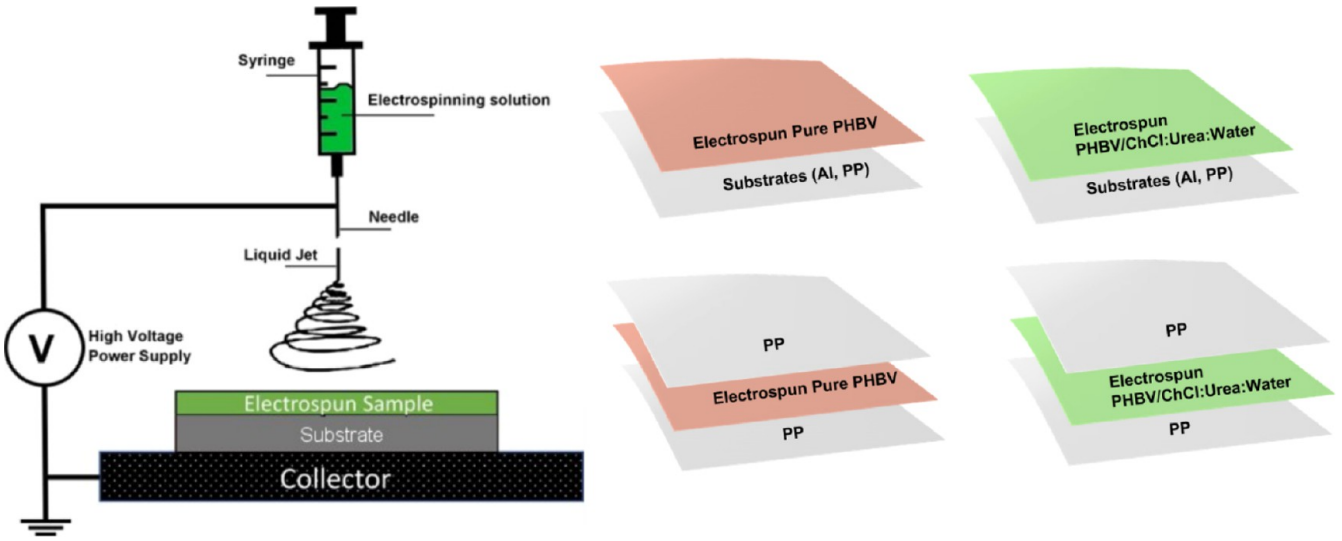

Figure 1. Schematic illustration of prepared samples by electrospinning.

stainless-steel needle (internal diameter of 0.7 mm) injector placed vertically toward a grounded flat collector. The distance between the needle and the collector was set at 15 cm. The NADES-containing PHBV fibers were optimally produced using a positive voltage of 17 kV and a flow rate of 0.5 mL/h per needle. In the case of the optimal processing of the pure PHBV fibers, only the flow rate of 6 mL/h was different. For both, a negatively polarized collector was used at −3 kV. The electrospinning process was performed in an enclosed chamber, being the ambient parameters controlled. Temperature and humidity were set to 25 °C and 50% RH to simulate the ambient conditions in the air-conditioned lab and to 35 °C and 20% RH for dry conditions, respectively. Unless otherwise stated, all the electrospinning processes were carried out in ambient conditions (25 °C and 50% RH). The process parameters were optimized to get a stable Taylor cone, which ensures stable processing. Fibers were collected on different substrates, namely, aluminum (Al) foil and non-woven spunbond polypropylene (PP), within the range of 0.1−15 and 25 g of fibers per square meter (GSM) sample area. The electrospinning process and sample preparation are illustrated in Figure 1. A multilayer strategy was also studied. This alternative configuration was obtained by placing another PP layer on top of the electrospun PHBV/ChCl/urea/water deposited on PP and compared with the multilayer strategy made of pure PHBV fibers just deposited on PP.

2.4. Characterizations. *2.4.1. Characterization of Electrospinning Solutions.* Electrospinning solutions were characterized in terms of viscosity, surface tension, and conductivity. The viscosity was measured using Fungilab Visco Basic Plus (Barcelona, Spain). The surface tension was measured using the Wilhelmy plate method in the Krüss GmbH EasyDyne K20 tensiometer (Hamburg, Germany). The conductivity measurements were performed using Hanna Instruments HI98192 conductivity probe (Gothenburg, Sweden). All the measurements were carried out in triplicate at room temperature.

2.4.2. Morphology. The morphology of the electrospun fibers was examined by scanning electron microscopy (SEM). The SEM micrographs were taken using a Hitachi S-4800 electron microscope (Tokyo, Japan), and for low magnification pictures, the Philips ESEM XL30 electron microscope (Amsterdam, Netherlands) at an accelerating voltage of 5 kV and a working distance of 8 mm. The samples were fixed to holders using conductive double-sided adhesive tape and sputtered with a mixture of gold-palladium for 2 min under vacuum prior to observation. The average fiber diameter was determined via the ImageJ Launcher software program [(NIH) (Bethesda, MD, USA)] from the SEM micrographs in their original magnifications. Fiber orientation was analyzed using the OrientationJ plugin to the ImageJ (NIH) software.[34]

2.4.3. EDX Analysis. The chemical composition of the electrospun PHBV/ChCl/urea/water fibers was analyzed and visualized using an energy-dispersive X-ray (EDX) detector (Oxford Instruments, Oxfordshire, UK) coupled to a Philips ESEM XL30 electron microscope (Amsterdam, Netherlands) at an accelerating voltage of 20 kV.

2.4.4. Electrostatic Charge Measurements. The electrostatic charges on the samples were measured using an SMC IZH10 electrostatic meter (Tokyo, Japan). For the measurement, samples of 5 × 5 cm were placed on paper, and the electrical potential (static voltage) was measured 1 cm away from the sample surface. The equipment was set to the maximum value reading mode, and at least 10 measurements were done for each sample. The value presented is the average and standard deviation of these 10 measurements.

2.4.5. Charge Stability under Different Storage Conditions. The stability of the electrical charge under different storage conditions was also studied. The storage conditions selected for this study were different RHs since humidity is one of the main parameters affecting charge stability,[8] that is, 0, 50, and 84% RH. To study the effect of humidity, the samples were stored at 25 °C in the air-conditioned lab at 50% RH, and in desiccators at 25 °C with silica gel for 0% RH, and with a saturated solution of potassium chloride for ca. 84% RH. For this experiment, all of the electrospun fibers were deposited on PP at 1 GSM. The charge stability of the PHBV fibers containing NADES was compared with the charge stability of the pure PHBV fibers, as well as neat PP as a control. Finally, the charge stability on a multilayer system was also studied only at the monitored lab ambient conditions, that is, 25 °C and 50% RH. For this, another layer of non-woven PP was placed on top of the electrospun PHBV/ChCl/urea/water fibers deposited on non-woven PP at 1 GSM, and the same

https://doi.org/10.1021/acsomega.2c05838
ACS Omega 2023, 8, 3798−3811

multilayer system for pure PHBV fibers was used as a control group. Charge stability studies were performed as a function of storage time of up to 7 days, and time 0 measurements were taken immediately after the electrospinning process.

2.5. Filtration Performance. The filtration and breathing resistance performance of the filter media developed were measured using procedures gathered within the European EN149:2001 + A1:2009 standard using a Filter Media Test Rig PMFT 1000 M (Palas, Germany). The penetration test was carried out with a paraffin oil aerosol with particle sizes spanning from ca. 0.14 to 4 μm, after 3 min of aerosol exposure. The pressure drop of the samples, also named in this work as breathing resistance, was measured by passing compressed air through the filter at flow rates of 160 L/min, simulating extreme exhalation within the above EN149 standard, and expressed in Pa. The dimension of the samples measured was 100 cm^2, and the testing conditions were 25 °C and 50% RH.

2.6. Corona Treatment. To induce the generation of charges on the nanofibers, the materials were treated using a TANTEC series no. CGC/30N system. Corona treatment is based on high-frequency discharges that create charges in the material and increase its surface energy. The charging bar was placed above the sample at a distance of approximately 5 cm from the surface of the nanofibers at a voltage of 18−20 kV for 10 min after having placed the sample on a drum which was rotating at a controlled speed of 100 rpm.

3. RESULTS AND DISCUSSION

3.1. Solution Characterization. It is well understood that the morphology and electrospinnability of the materials are highly dependent on the physical characteristics of the initial polymeric solution, such as viscosity, surface tension, and electrical conductivity.[35] The solution properties of pure PHBV, ChCl/urea/water (NADES), and PHBV/ChCl/urea/water solutions were reported in Table 1. As it can be seen from the table, the PHBV/ChCl/urea/water solution exhibited a significantly higher electrical conductivity (2595 ± 31 μS) compared to the pure PHBV solution (4.00 ± 0.02 μS). This could be mainly attributed to the presence of NADES since the conductivity of neat NADES (ChCl/urea/water) was found to be 4153 ± 32 μS, in agreement with data previously reported by Du et al.[36] In the case of surface tension, although the surface tension of ChCl/urea/water was higher than the surface tension of the pure PHBV solution, the incorporation of NADES into the PHBV solution provoked only a slight increase in surface tension up to 22.8 mN/m, which did not affect the electrospinnability of the PHBV/ChCl/urea/water solution. On the other hand, the average viscosity of pure PHBV solution decreased with the incorporation of NADES from 571.5 to 442.2 cP (Table 1).

Table 1. Solution Properties of PHBV, ChCl/Urea/Water, and PHBV/ChCl/Urea/Water Solutions

solutions	viscosity (cP)	surface tension (mN/m)	conductivity (μS/cm)
pure PHBV	571.5 ± 2.1	21.2 ± 0.1	4.00 ± 0.02
ChCl/urea/water	474.0 ± 3.3	68.1 ± 0.1	4153 ± 32
PHBV/ChCl/urea/water	442.2 ± 1.8	22.8 ± 0.1	2595 ± 31

3.2. Effect of NADES on the Morphology of PHBV Fibers. Next, the electrospinnability of the PHBV/ChCl/urea/water solution was evaluated, and the characteristics of the obtained fibers were compared to those of pure PHBV fibers. For the purpose of comparison, a fiber mat of 25 GSM was produced using an Al foil substrate for both samples. The SEM micrographs of the obtained electrospun fibers of both materials are shown in Figure 2a,b, respectively. Pure PHBV produced smooth and inter-fused fibers without the presence of beads and with a mean fiber diameter of 884 ± 259 nm (Figure 2a). This result is in concordance with the morphological results previously reported by Figueroa-Lopez et al.[16] and Melendez-Rodriguez et al.[27] for the same polymer. More interestingly, the incorporation of NADES (ChCl/urea/water) into PHBV fibers resulted in a smooth, continuous, more oriented (see below for the specific discussion), and bead-free fiber morphology with an average fiber diameter of 303 ± 62 nm (Figure 2b). This reduction in fiber diameter can be explained by the higher conductivity of the PHBV/ChCl/urea/water electrospinning solution, as shown in Table 1, since a higher solution conductivity has been reported to lead to smaller fiber diameters.[37] For instance, Chen et al. obtained thinner PHBV fibers from an electrospinning solution with increased conductivity due to the addition of nanoparticles, which was poly(*N*,*N*-dimethylaminoethylmethacrylate grafted onto cellulose nanocrystals.[38] Khatri et al. also reported smaller diameters when electrospinning zein nanofibers with choline chloride/furfuryl alcohol (2:1) than with pure zein.[33]

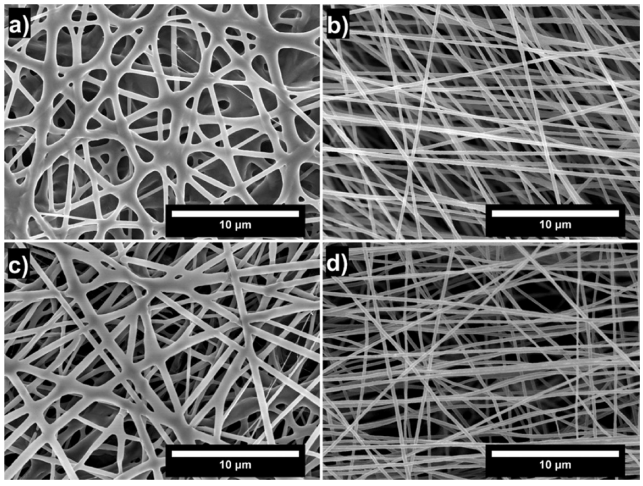

Figure 2. SEM micrographs of 25 GSM of (a) electrospun pure PHBV on an Al foil, (b) electrospun PHBV/ChCl/urea/water on an Al foil, (c) electrospun pure PHBV on PP, and (d) electrospun PHBV/ChCl/urea/water on PP at 25 °C and 50% RH. Scale markers are of 10 μm.

Additionally, this effect of fiber diameter reduction was also observed when depositing the fibers on a different substrate, the selected model substrate material made of non-woven spunbond PP in this case, being the obtained fiber diameters of 781 ± 223 and 288 ± 35 nm for pure PHBV and PHBV/ChCl/urea/water fibers, respectively (Figure 2c,d).

In order to determine the presence and distribution of the added NADES within the PHBV fiber mats, fiber samples were subjected to EDX analysis. As it can be seen from the Figure 3, the EDX spectrum revealed the presence of C and O as major elements (60.3 and 36.5 wt %, respectively), together with Cl

https://doi.org/10.1021/acsomega.2c05838
ACS Omega 2023, 8, 3798−3811

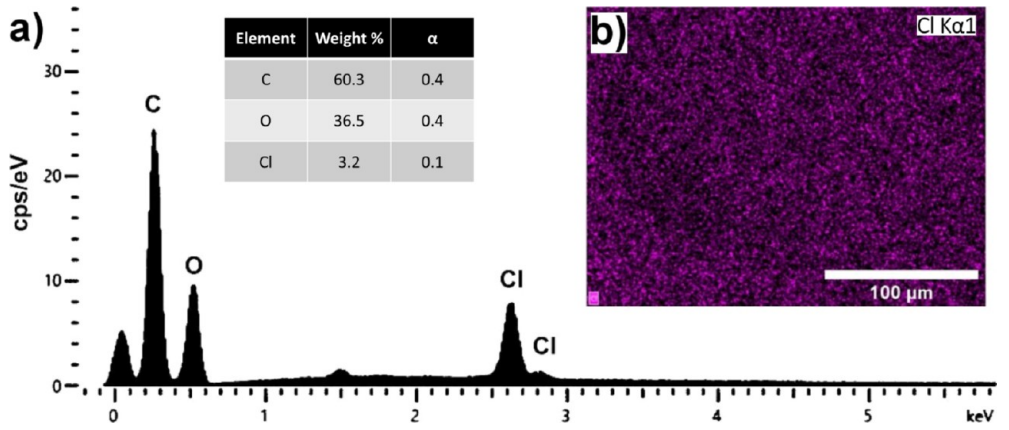

Figure 3. EDX analysis: (a) EDX scan spectrum and (b) elemental mapping for Cl of 25 GSM electrospun PHBV/ChCl/urea/water fibers on an Al foil. Scale marker is 100 μm.

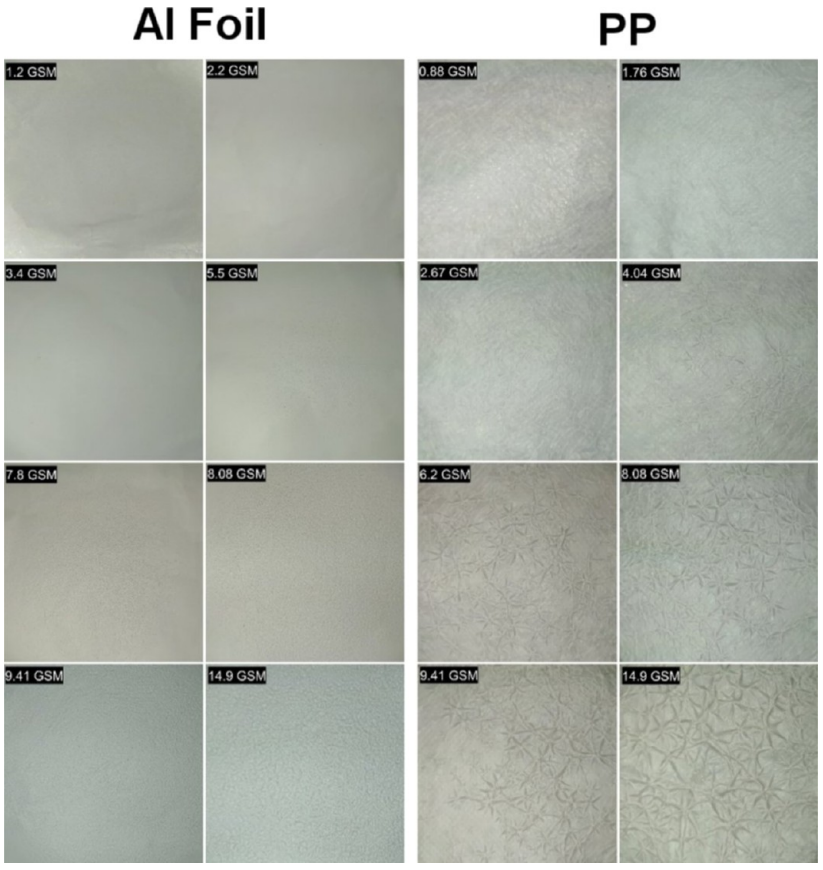

Figure 4. Photographs of the produced PHBV/ChCl/urea/water samples on an Al foil (left) and PP (right) with rugose surfaces at different grammages. All the samples were prepared at 25 °C and 50% RH.

in smaller quantities (3.2 wt %), arising from ChCl/urea/water. Furthermore, the elemental mapping of PHBV/ChCl/urea/water fiber mats (Figure 3b), which were performed selecting the element Cl, shows a relatively homogenous distribution of the NADES, ChCl/urea/water, within the PHBV fibers. Thus, one can infer from these results that the NADES, ChCl/urea/water, is homogeneously present within the PHBV fibers.

However, the real surprising fundamental effect of adding NADES to the formulation was the macroscopic observation of the creation of a certain rugosity on the deposited mat of nanofibers that was produced only under certain experimental conditions (see Figure 4). From this figure, it can be observed that the electrospinning of PHBV/ChCl/urea/water on Al foil resulted in samples with a rugose surface morphology when the deposited grammages were equal to or higher than 7.8 GSM. However, when PP was used as a substrate, star-shaped rugosities were also observed but even at the lowest grammages used, which increased in size and visibility as the grammage increased. Interestingly, the cited rugosity was not observed when depositing the pure PHBV on any of the two substrates, even at grammages of 25 GSM, hence resulting in the expected flat and homogeneous fiber mats.

https://doi.org/10.1021/acsomega.2c05838
ACS Omega 2023, 8, 3798−3811

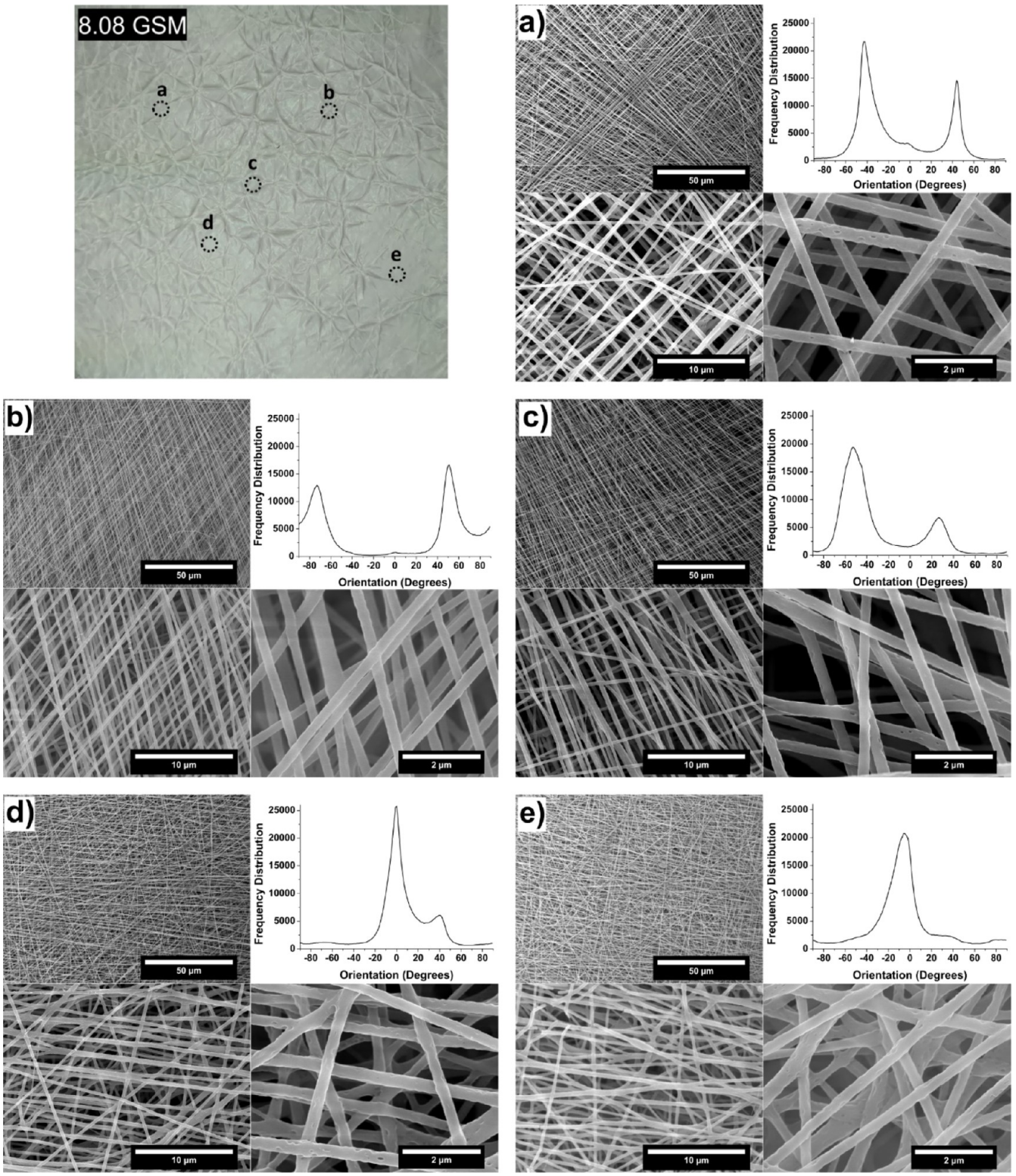

Figure 5. SEM micrographs and orientation frequency as a function of angle plots of different regions (a−e) of the electrospun PHBV/ChCl/urea/water on PP. Areas of interest are shown on the optical image of the sample (top-left). Scale markers are of 50, 10, and 2 μm.

Additionally to the macroscopic effect on morphology, the addition of NADES provoked interesting microscopic effects as shown in Figure 5. It was observed that these macroscopic rugose areas were made of naturally aligned microscopic structures. Figure 5 displays the micrographs taken from different areas of the electrospun PHBV/ChCl/urea/water sample with 8.08 GSM over PP, and the corresponding plots represent the orientation frequency of the fibers deposited at different angles for the areas of interest. The height and width of the peak are measurements of the degree of the fiber alignment seen in the SEM images; thus, whereas shorter and broader peaks indicate a lower degree of alignment, higher and

https://doi.org/10.1021/acsomega.2c05838
ACS Omega 2023, 8, 3798−3811

narrower peaks indicate a greater degree of alignment.[39] As it can be seen from the micrographs and plots, all areas exhibited fiber alignment on non-woven PP. However, the orientation of the alignment was found to be dependent on different regions of the sample surface. The regions close to the "*mountains*" of the star-shaped rugosity (Figure 5a−c) exhibited an orientation with two distinct peaks indicating an orthogonal fiber orientation. On the other hand, the flatter regions or valleys (Figure 5d,e) displayed one-direction alignment, showing only one dominant peak. In addition, similar results were observed for the PHBV/ChCl/urea/water fibers deposited on Al foil in terms of fiber alignment; however, no particular trend was identified as the size of the characteristic shapes causing rugosity were notably smaller (results not shown).

Moreover, it was found out that the appearance of rugosity in the fiber mat was also dependent on the ambient humidity during the electrospinning process. Thus, Figure 6 shows, as an example, the macroscopic photographs and SEM images taken at 35 °C and 20% RH on the electrospun PHBV/ChCl/urea/water fibers deposited on Al foil with grammages of 25 GSM. As it can be seen from the images, flat and smooth electrospun mats with an average fiber diameter of 556 ± 90 nm without any rugosity were obtained.

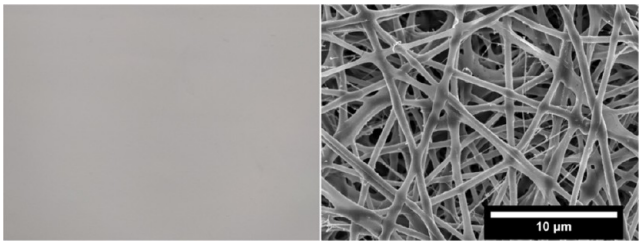

Figure 6. Photograph (left) and SEM micrograph (right) of PHBV/ChCl/urea/water fiber mats of 25 GSM electrospun at 35 °C and 20% RH.

It was observed that rugous electrospun PHBV/ChCl/urea/water fibers deposited on different substrates, that is Al foil and PP, showed a charge retention behavior as a function of grammage. Charges were measured 24 h after electrospinning. As it can be seen from the observation of Figure 7, the charge retention profile of the samples exhibited considerably different trends depending on the substrate. The electrospun PHBV/ChCl/urea/water fibers deposited on Al foil with grammages lower than 5.5 did not exhibit any charge retention, whereas after this point, an increase in residual charges was observed with the increase in grammage. Moreover, PHBV fibers containing NADES showed positive charge retention at any grammages used when deposited on PP. The PP substrate was also tested after exposure to the same electrospinning conditions as the polymer solutions for up to 5 min and provided a small but measurable charge retention, indicating that the substrate can also get small residual charges in an agreement with previous studies.[40,41] A sample of 25 GSM of pure PHBV deposited on the PP substrate was also produced, delaminated from the PP and tested for residual charges 24 h after and showed no charges. Furthermore, the grammages at which the residual charges were first observed in the samples deposited on Al foil coincided with the grammages at which the rugosity began to be detected, that is, 7.8 GSM in Figure 3.

To the best of our knowledge, the above-stated events of rugosity, fiber alignment, and charge retention when electrospinning polymers containing NADES have not been reported before. However, the formation of three-dimensional (3D) features in electrospun fiber mats has been reported by previous authors in different polymeric systems. Bonino et al. reported the formation of 3D structures when electrospinning an aqueous solution of polyethylene oxide and alginate.[42] To explain this phenomenon, they proposed a mechanism based on fiber−fiber repulsions caused by the surface charges of a negatively charged high charge density material, in their case sodium alginate. The negatively charged groups of the alginate were populated on or near the surface of the electrospun fibers due to the attractive forces in the applied positive electric field.

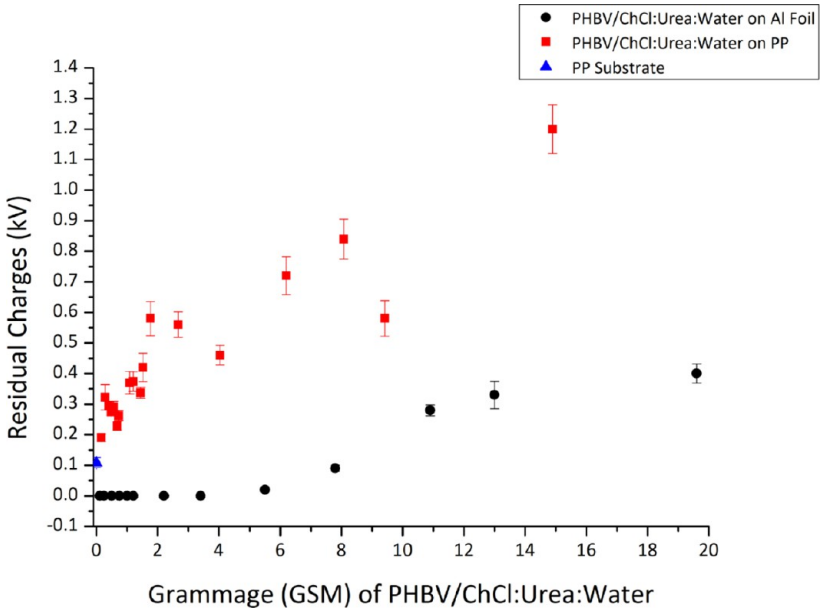

Figure 7. Charge retention capacity after 24 h of storage time of electrospun PHBV/ChCl/urea/water fibers deposited at 25 °C and 50% RH on an Al foil and PP as a function of grammage. The charge retention of the PP substrate is also included as control.

https://doi.org/10.1021/acsomega.2c05838
ACS Omega 2023, 8, 3798−3811

As a result, the fibers became predominantly negatively charged surfaces and experienced repulsion forces between adjacent fibers, causing them to protrude away from the collector plate to form 3D structures. However, these authors did not report any charge retention.

Another example is the work of Cai et al., who produced 3D electrospun fiber mats from a solution consisting of sodium dodecyl sulfate (SDS) containing zein solubilized in 70% aqueous ethanol.[43] They reported that the formation of 3D structures was attractive and repulsion forces driven. Briefly, the surface conductivity of the polymer increased due to the population of SDS on the surface of the fibers, and when these fibers stroke the oppositely charged collector (attractive forces), they lose their opposite charges and become charged with the collector's charge, resulting in fibers being repelled from the collector and the formation of the 3D structures. However, it should be noted that the resulting structure had a fluffy appearance, with no residual charges or alignment being reported.

In regard to 3D structures having reported residual charges, Vong et al. obtained 3D polystyrene fibers with phosphoric acid as an additive.[44] It was reported that the obtained 3D structures were obtained due to the attractive forces between the positively charged injector and the negatively charged fibers due to the polarization and charge inductions of the collector. However, their 3D fiber mat was spongy, soft, and made of randomly oriented fibers. Additionally, they reported charge retention for 12 h, resulting in fibers being attracted by a charged rod.

In our opinion, neither the previous mechanisms nor the features reported explain completely our observations. According to our hypothesis, the here-observed rugosity could be related to the measured residual charges, shown in Figure 7. The accumulation of positive residual charges must be associated with the presence of NADES and their polarization ability under external electrical fields, such as during the electrospinning process, which leads to an increase in molecular dipole moment, as well as ion−dipole and dipole−dipole interaction energies of DES species.[45] As a result of the polarization in a positively charged electrical field, the DES molecules were thought to create permanent dipoles with a net positive charge.[46−48] As demonstrated in Figure 3, NADES were homogeneously distributed along the fiber, which was also supported by SEM observations of the cryofracture of the fibers (Figure 8b). As shown in the figure, the fibers exhibited a rough surface and a porous structure within the fibers. This surface roughness structure was not observed in the pure PHBV fibers. The cited morphology must then be attributed to NADES domains, whereas the voids observed inside the fibers indicate NADES being entrapped, which could promote charge accumulation since the polymer could act as a rigid insulating interface[49,50] preventing charge dissipation.

For the formation of the here-observed rugosity, we hypothesized that the base layer of fibers was able to only partially dissipate its charges when reaching the substrate connected to the negatively polarized collector. For this reason, as grammage increased, the accumulated charge increased, preventing charges from the following layer of fibers to be dissipated through the negatively polarized collector and causing fibers to protrude from the surface of the mat, as a consequence of interfiber repulsion, forming the observed rugose morphology. As the peak height increases, the electrical field between the needle and the mountain peak also changes, causing localized regions of a higher repulsion electric field, which leads to subsequent fibers to land in the vicinity of the peaks. Furthermore, some other formations evolve as layers of fiber connect the neighboring peaks, creating ridges around the peaks, forming the morphologies shown in Figure 8a.

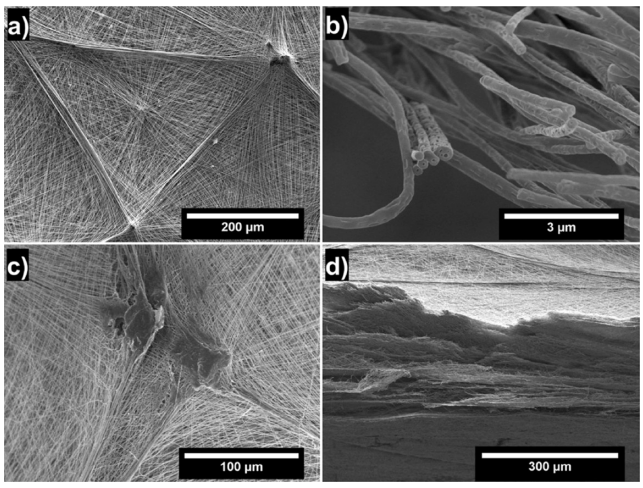

Figure 8. SEM micrographs: (a) characteristic cellular rugosity morphology, (b) cross-section and surface morphology of fibers obtained from the rugose area, (c) tip of a peak and ridges on the rugose area, and (d) cross-section of a rugose mat. Images were taken for a 14.9 GSM electrospun PHBV/ChCl/urea/water fiber sample on PP at 25 °C and 50% RH. Scale markers are 200, 3, 100, and 300 μm for (a−d), respectively.

As demonstrated in Figure 4, deposition of 7.8 GSM of PHBV/ChCl/urea/water fibers on a conductive Al foil substrate was required to observe rugosity, most likely due to the higher conductivity of Al foil. However, when the less conductive PP was used as the substrate, the charge dissipation was more difficult already from the lowest grammages as discussed above, causing the rugosity to appear even at GSM as low as 0.88. A similar trend can also be observed in terms of charge retention properties as a function of GSM and substrate (see Figure 7).

As stated before, the rugose structures were only obtained for electrospinning of PHBV/ChCl/urea/water at the controlled ambient conditions, where the RH was 50%. It has been previously reported in a review paper by Mailley et al. that RH is a critical variable to modify the morphology of the formed electrospun mats.[51] Thus, it was reported that hydrophobic polymers are prone to rapid solidification under high humidity. This is because the presence of water in the jet acts as an anti-solvent for the hydrophobic polymer and causes rapid solidification due to precipitation.[51] Hence, we hypothesized in this study that such an effect of rapid fiber solidification can also occur in the hydrophobic PHBV fibers. When the jet solidifies rapidly, some of the NADES are retained charged inside the fibers. Additionally, rapidly solidified fibers could provide enough strength to support a 3D configuration.[52] Another factor of humidity is its ability to promote polarization. At high humidity, a great number of water molecules get polarized, and thus, enhances nanofiber dipole formation, consequently leading to a high net capacitance of the fiber mats.[53]

Under dry conditions (20% RH, 35 °C), electrospun PHBV/ChCl/urea/water fiber mats exhibited no rugosity

https://doi.org/10.1021/acsomega.2c05838
ACS Omega 2023, 8, 3798−3811

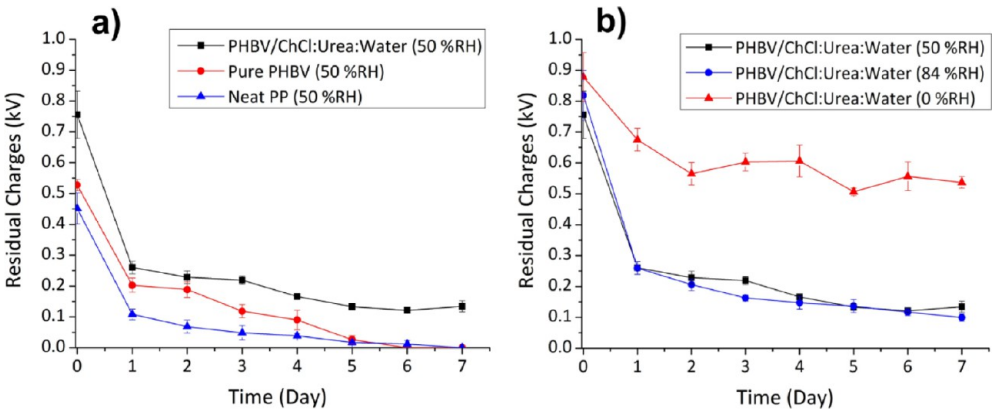

Figure 9. Residual charges as a function of storage time of 1 GSM of (a) electrospun PHBV/ChCl/urea/water on PP, electrospun pure PHBV fibers on PP, and the substrate PP at 25 °C, 50% RH; (b) electrospun PHBV/ChCl/urea/water fibers on PP at 25 °C and under different RH conditions of 0, 50, and 84%.

even at grammages of 25 GSM (see left Figure 5). Under these conditions, the solidification of the polymer is not so fast, resulting in wetter fibers with higher charge dissipation ability, which in turn result in conventional flat fiber 2D mat structures.

Another interesting feature that we noticed is the fact that above a certain grammage, top layer fibers of the peaks and ridges seemed merged (Figure 8c). This indicates that when peaks and/or ridges have enough height, subsequent fibers tend to land on these structures somewhat wet. This might be due to changes in whipping instabilities caused by the localized high electric field originating from the peaks and ridges.[54] In addition to the described observations, Figure 8d also shows that a low density of fiber packing, caused by the repulsion forces between the different adjacent fiber layers, has taken place.

Finally, all macroscopic rugose areas exhibited natural fiber alignment along the peaks and ridges, as shown in Figure 5, since the rugose surface of mats could provoke changes in the electric field in the vicinity of the collector, resulting in a patterned distribution of the electric field over the patterned structure of the rugose substrate that promotes the in situ fiber alignment.[55−57] The electrostatic repulsions between the upcoming and deposited fibers can further promote the fiber alignment.[58] In addition, the fibers suspended across the gap can remain highly charged after deposition due to the lack of contact with the collector. As expected, fiber alignment was only observed for the electrospinning of PHBV/ChCl/urea/water, pure PHBV fibers did not exhibit any rugosity or fiber alignment.

3.3. Electrostatic Charge Stability under Different Storage Conditions. In additional experiments and in filtration applications where typically low GSM coating of nanofibers are often used,[59,60] the electrostatic charge stability of 1 GSM of electrospun PHBV/ChCl/urea/water fibers deposited on top of PP was investigated under different storage conditions, and the results are displayed in Figure 9a,b, in comparison with the control materials (pure PHBV fibers on the PP substrate and the substrate of PP).

As it can be seen from Figure 9a, all samples exhibited some residual charges at time 0, including the PP substrate and the pure PHBV fibers deposited on PP. In this study, it was previously discussed that pure PHBV fibers did not show any charge retention when deposited on conductive Al foil, and this was also the case when delaminated from the PP substrate. The fact that somewhat higher charges were recorded during the first days of storage in the pure PHBV fibers compared to the neat PP substrate could arise from the pure PHBV fibers acting as an extra layer to handicap charge dissipation from the PP. Charges on PP are known to dissipate over time at ambient conditions,[4,40] yet this process can be reduced by the addition on top and below of additional layers.[61]

In Figure 9a, it becomes clear that PHBV/ChCl/urea/water fibers exhibited an approximately 50% higher charge at time 0 compared to the initial charges of electrospun pure PHBV fibers and neat PP. This is ascribed to the electrostatic charge retention contribution of the NADES itself, as discussed above. As previously demonstrated in Figure 7 and discussed above, the incorporation of NADES into PHBV fibers resulted in charged fibers. After 24 h, a rapid charge decay was seen for all the samples, indicating that the higher initial charge is dissipated at the 50% RH from the surface or shallow trap sites of the samples.[4,62] Among all the samples in Figure 9a, non-woven neat PP exhibited the fastest and highest charge loss, almost reached 0 kV on the fifth day, and displayed no residual charges on the sixth and seventh days. Furthermore, a similar trend was observed for the electrospun pure PHBV fibers. However, electrospun PHBV/ChCl/urea/water fibers showed a retained residual charge plateau after day five. This could be explained again by the persistent charges localized within the deeper trap sites of the PHBV/ChCl/urea/water fibers, even at 1 GSM.

Figure 9b shows the electrostatic performance of electrospun PHBV/ChCl/urea/water fibers under different conditions of 0% RH, 50% RH, and 84% RH for 7 days of storage time. As it can be seen from the figure, the fibers exhibited a similar trend at 50% RH and 84% RH conditions. However, at 0% RH, a drastic difference appeared, showing persistently high charges within the electrospun PHBV/ChCl/urea/water fibers. This is explained by the well-known charge-dissipating effect of humidity. When the environment is humid, water molecules may sorb and diffuse within the fibers, acting as a carrier of the trapped charges, which increase the charge migration and accelerate the decay.[1,63]

To protect the electrostatic stability of the materials from the environment's humidity, a multilayer configuration was used.[61] To do this, the electrospun PHBV/ChCl/urea/water fiber mat deposited on a non-woven PP was protected by

https://doi.org/10.1021/acsomega.2c05838
ACS Omega 2023, 8, 3798−3811

placing another similar layer of PP on top of the electrospun fibers, and the pure PHBV fibers were used again as a control (see schematics in Figure 1). As demonstrated in Figure 10, the multilayer approach resulted in a steady charge retention profile for 7 days. More importantly, the electrostatic charge retention of PHBV/ChCl/urea/water fibers was noticeably higher than that of the pure PHBV fibers, showing almost twice higher than that of the control for 7 days. Hence, this is again attributed to the charge-accumulation contribution of the NADES.

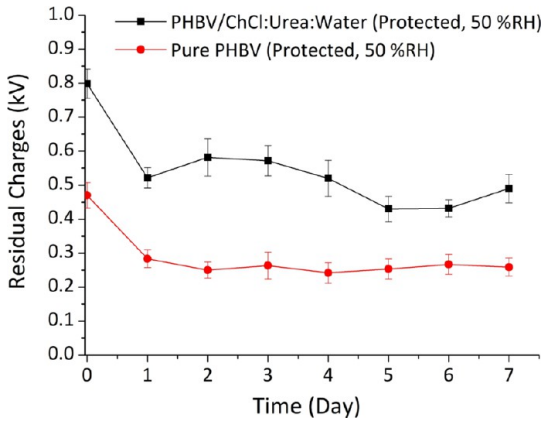

Figure 10. Evolution of the residual charges as a function of storage time for the multilayer approach of 1 GSM electrospun PHBV/ChCl/urea/water fibers sandwiched between PP layers and for the multilayer approach of 1 GSM electrospun pure PHBV fibers sandwiched between PP layers at 25 °C and 50% RH.

3.4. Assessing PHBV/ChCl/Urea/Water Electrospun Fibers in Filtration. Electrospun fibers have attracted a large attention in the area of filtration since the technology provides a high filtration efficiency at very low material grammages, which allows the use of very little material to generate highly efficient filter materials.[64] The interesting characteristics of the developed nanofibers with charge retention properties may lead to an increase in filtration efficiency while unaltering pressure drop. For this reason, and based on our own previous research, the nanofibers were deposited over PP and configured in a multilayer structure with the optimum material configuration for filtration strategies.[29] As described in Figure 11a, this multilayer structure consisted of two layers of PP of 17 GSM on the exterior and interior, and two symmetric layers in the middle of electrospun PHBV/ChCl/urea/water totaling 0.3 GSM, and a similar structure but based on a pure PHBV fiber layer without NADES as a control.

The performance of the air filters is closely related to the structural factors of the nanofiber membrane, such as fiber

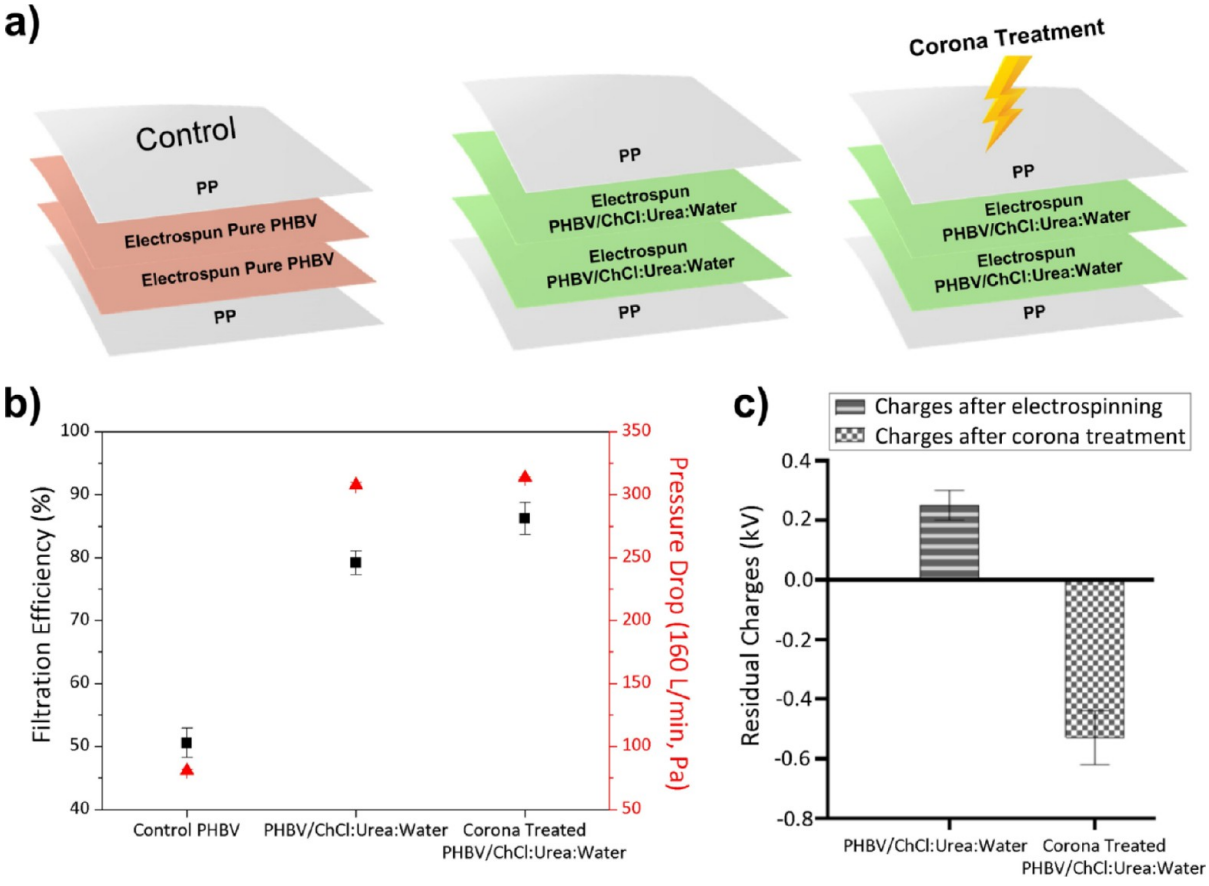

Figure 11. (a) Schematic illustration of the multilayer approach formed by two layers of PP of 17 GSM sandwiching two layers of pure PHBV or PHBV/ChCl/urea/water fibers (PP/0.15/0.15/PP). (b) Pressure drop and filtration efficiency measured 1 day after electrospinning for the multilayer structure composed of pure PHBV, PHBV/ChCl/urea/water, and corona-treated PHBV/ChCl/urea/water samples. Pressure drop was measured with an air flow rate of 160 L/min. (c) Residual charges of PHBV/ChCl/urea/water fibers 1 day after electrospinning and after corona treatment. Charges were measured in half of the sandwich (PP/nanofibers 0.15).

https://doi.org/10.1021/acsomega.2c05838
ACS Omega 2023, 8, 3798−3811

morphology and diameter, porosity, grammage, orientation, and so forth,[65] as well as charge retention in the case of electret fibers, which enables an electrostatic role of particle capturing to the overall filtration performance.[7] Figure 11b shows that the multilayer structure of the control PHBV sample exhibited a paraffin aerosol filtration efficiency of 50.56 ± 2.33% with a pressure drop of 80.83 ± 1.09 Pa. For the same grammage, the results were significantly different for the PHBV-containing NADES sample (PHBV/ChCl/urea/water), having a paraffin aerosol filtration efficiency of 79.19 ± 1.89% and a pressure drop of 307.57 ± 2.22 Pa. As discussed in Section 2.2, PHBV/ChCl/urea/water fibers showed a fiber diameter of approximately 290 nm, whereas pure PHBV fibers had an average fiber diameter of ca. 780 nm with inter-fused fiber morphology. Thus, compared to pure PHBV, a higher filtration efficiency for PHBV/ChCl/urea/water was expected since the addition of NADES resulted in a lower fiber diameter, which in turn means a lower pore size,[66] and higher residual charges, which eventually led to higher filtration efficiencies and pressure drop in the NADES-containing filter.[7,67]

Since the GSM deposited were rather low, to avoid a too-high pressure drop and to check how a higher charge could affect the filtration performance, a corona post-treatment was applied to the material with NADES. Figure 11c shows the residual charges of the PHBV/ChCl/urea/water sample measured one day after electrospinning (+0.25 ± 0.05 kV) and after corona treatment (−0.53 ± 0.09 kV). The PHBV fibers containing NADES exhibited significantly improved charge retention capacity after the corona treatment. For the case of the pure PHBV fibers, there were smaller differences in residual charges, being before the corona treatment of +0.15 ± 0.02 kV and after the corona treatment of −0.16 ± 0.02 kV. As a result, the corona treatment further increased the filtration efficiency of the PHBV/ChCl/urea/water sample by approximately 7% with only a small increase in pressure drop (Figure 11b).

Air filter media are generally made of chemically synthesized or petroleum-based raw materials, such as polypropylene.[12] Meantime, researchers are still endeavoring for the design and development of innovative biobased organic recyclable nanofiber filtration membranes to fabricate highly efficient filtration systems with potentially lower carbon footprint.[12,68,69] Additionally, many attempts have been made to functionalize conventional synthetic or natural polymers through specific additives to enhance their filtration performance or functionality; however, these additives can be expensive.[12,68] Hence, the development of filtration membranes made of a natural microbial biopolymer having excellent biocompatibility and biodegradability characteristics, and making it a strong candidate to be used in air filtering applications by incorporating cheap and green NADES, is expected to add significant value to the vibrant field of air filtration applications. Herein, it was demonstrated for the first time that NADES, which has numerous and unexplored potential applications, could play a new application role in improving filtration efficiency for biopolymers such as PHBV.

4. CONCLUSIONS

Pure and NADES-loaded PHBV fibers were prepared by electrospinning, and solution characterizations were performed in terms of viscosity, surface tension, and conductivity. Data suggested that the incorporation of NADES caused an increase in solution conductivity of approximately 650-fold. The morphology of the here-prepared electrospun fibers containing NADES was examined by SEM and macroscopically. SEM images showed that straight, bead-free morphology with fiber diameters in the nanoscale (approximately 300 nm) were produced. The chemical composition of PHBV/ChCl/urea/water fibers was analyzed by EDX, and it was seen that ChCl/urea/water was homogeneously distributed within the PHBV fibers. Macroscopically, the incorporation of NADES into PHBV fibers resulted in an unreported 3D rugose surface of the prepared mats when electrospun at 50% RH. A repulsion force-driven mechanism due to NADES polarization ability was proposed for the formation of the rugose 3D fiber mats. Charge measurements showed that PHBV/ChCl/urea/water fibers exhibited the capacity to retain electrical charges on conductive Al foil starting at grammages above 5.5 GSM and on the less-conductive PP at the lowest grammages studied. Fibers on the rugose area were deposited in an aligned manner. The 3D rugose morphology was not seen in the PHBV/ChCl/urea/water fibers when this material was electrospun at 20% RH, suggesting that the effect is connected with rapid fiber solidification, thought to occur at higher RHs. The 3D rugose morphology was also not seen in the pure PHBV fibers. Charge stability studies were performed for 1 GSM electrospun PHBV/ChCl/urea/water fibers on PP under different RH storage conditions. According to the results, PHBV/ChCl/urea/water fibers on PP showed a plateau of retained charges under ambient conditions, 25 °C and 50% RH, after 5 days, whereas the residual charges recorded on neat PP and pure PHBV fibers on PP disappeared completely after 5 days. Also, the studies performed under different RHs showed that the residual charges decayed more easily at medium (50% RH) and high RH conditions (80% RH), compared to dry conditions (0% RH). Finally, to prevent or slow the charge decay on the fibers, a multilayer approach was developed by adding an extra layer of PP. The results showed that the best electrostatic performance was found for protected electrospun PHBV/ChCl/urea/water fibers, with the highest electrical potential of 0.80 ± 0.04 kV at time 0 and 1 GSM and the lowest residual charge reduction of 38.6% after 7 days of storage time under ambient conditions. The use of a multilayer structure in which a double layer totaling 0.3 GMS of PHBV/ChCl/urea/water fibers was used showed a significant improvement in filtration efficiency, which was increased from 50.56 ± 2.33% to 79.19 ± 1.89% by the addition of NADES into PHBV fibers. This was improved further after corona charging treatment by approximately 7% with only a small increase in pressure drop. According to these results, the here-developed NADES-containing PHBV fibers with charge retention capacity can be considered as a very interesting and promising new electret material for air filtration and potentially for other applications such as in tissue engineering, for retaining and controlled release of drugs, for power harvesting, and as sensors, microphones, transducers, field-effect transistors, and so forth.

AUTHOR INFORMATION

Corresponding Authors

Cristina Prieto − *Novel Materials and Nanotechnology Group, Institute of Agrochemistry and Food Technology (IATA), Spanish Council for Scientific Research (CSIC), Paterna 46980 Valencia, Spain;* orcid.org/0000-0002-0925-896X; Email: cprieto@iata.csic.es; Fax: (+34) 963 900 022

https://doi.org/10.1021/acsomega.2c05838
ACS Omega 2023, 8, 3798−3811

Jose M. Lagaron − *Novel Materials and Nanotechnology Group, Institute of Agrochemistry and Food Technology (IATA), Spanish Council for Scientific Research (CSIC), Paterna 46980 Valencia, Spain;* orcid.org/0000-0002-0502-359X; Email: lagaron@iata.csic.es

Authors

Ahmet Ozan Basar − *Novel Materials and Nanotechnology Group, Institute of Agrochemistry and Food Technology (IATA), Spanish Council for Scientific Research (CSIC), Paterna 46980 Valencia, Spain*

María Pardo-Figuerez − *Novel Materials and Nanotechnology Group, Institute of Agrochemistry and Food Technology (IATA), Spanish Council for Scientific Research (CSIC), Paterna 46980 Valencia, Spain*

Complete contact information is available at: https://pubs.acs.org/10.1021/acsomega.2c05838

Funding

This research was funded by the Spanish Ministry of Science and Universities (project RTI-2018-097249-B-C21) and the PTI + Global Health of CSIC.

Notes

The authors declare no competing financial interest.

■ ACKNOWLEDGMENTS

A.O. Basar wants to thank the Generalitat Valencia (GVA) for his Grisolía Fellowship (GRISOLIA/2020/19).

■ REFERENCES

(1) Liu, C.; Dai, Z.; He, B.; Ke, Q.-F. The Effect of Temperature and Humidity on the Filtration Performance of Electret Melt-Blown Nonwovens. *Materials* **2020**, *13*, 4774.

(2) Tsai, P. P.; Schreuder-Gibson, H.; Gibson, P. Different Electrostatic Methods for Making Electret Filters. *J. Electrost.* **2002**, *54*, 333−341.

(3) Li, Y.; Yin, X.; Si, Y.; Yu, J.; Ding, B. All-Polymer Hybrid Electret Fibers for High-Efficiency and Low-Resistance Filter Media. *Chem. Eng. J.* **2020**, *398*, 125626.

(4) Thakur, R.; Das, D.; Das, A. Study of Charge Decay in Corona-Charged Fibrous Electrets. *Fibers Polym.* **2014**, *15*, 1436−1443.

(5) Kravtsov, A.; Brünig, H.; Zhandarov, S.; Beyreuther, R. The electret effect in polypropylene fibers treated in a corona discharge. *Adv. Polym. Technol.* **2000**, *19*, 312−316.

(6) Cho, B. M.; Nam, Y. S.; Cheon, J. Y.; Park, W. H. Residual Charge and Filtration Efficiency of Polycarbonate Fibrous Membranes Prepared by Electrospinning. *J. Appl. Polym. Sci.* **2015**, *132*, 41340.

(7) Kilic, A.; Russell, S.; Shim, E.; Pourdeyhimi, B. The Charging and Stability of Electret Filters. *Fibrous Filter Media*; Elsevier Ltd, 2017, pp 95−121.

(8) Lee, J.; Kim, J. Material Properties Influencing the Charge Decay of Electret Filters and Their Impact on Filtration Performance. *Polymers* **2020**, *12*, 721.

(9) Liu, J.; Zhang, X.; Zhang, H.; Zheng, L.; Huang, C.; Wu, H.; Wang, R.; Jin, X. Low Resistance Bicomponent Spunbond Materials for Fresh Air Filtration with Ultra-High Dust Holding Capacity. *RSC Adv.* **2017**, *7*, 43879−43887.

(10) Wang, P. L.; Roschli, A.; Paranthaman, M. P.; Theodore, M.; Cramer, C. L.; Zangmeister, C.; Zhang, Y.; Urban, J. J.; Love, L. Recent Developments in Filtration Media and Respirator Technology in Response to COVID-19. *MRS Bull.* **2021**, *46*, 822−831.

(11) Xu, Y.; Zhang, X.; Hao, X.; Teng, D.; Zhao, T.; Zeng, Y. Micro/Nanofibrous Nonwovens with High Filtration Performance and Radiative Heat Dissipation Property for Personal Protective Face Mask. *Chem. Eng. J.* **2021**, *423*, 130175.

(12) Souzandeh, H.; Wang, Y.; Netravali, A. N.; Zhong, W. H. Towards Sustainable and Multifunctional Air-Filters: A Review on Biopolymer-Based Filtration Materials. *Polym. Rev.* **2019**, *59*, 651−686.

(13) Melendez-Rodriguez, B.; Reis, M. A. M.; Carvalheira, M.; Sammon, C.; Cabedo, L.; Torres-Giner, S.; Lagaron, J. M. Development and Characterization of Electrospun Biopapers of Poly(3-Hydroxybutyrate- Co-3-Hydroxyvalerate) Derived from Cheese Whey with Varying 3-Hydroxyvalerate Contents. *Biomacromolecules* **2021**, *22*, 2935−2953.

(14) Melendez-Rodriguez, B.; Torres-Giner, S.; Lorini, L.; Valentino, F.; Sammon, C.; Cabedo, L.; Lagaron, J. M. Valorization of Municipal Biowaste into Electrospun Poly(3-Hydroxybutyrate-Co-3-Hydroxyvalerate) Biopapers for Food Packaging Applications. *ACS Appl. Bio Mater.* **2020**, *3*, 6110−6123.

(15) Meereboer, K. W.; Pal, A. K.; Cisneros-López, E. O.; Misra, M.; Mohanty, A. K. The Effect of Natural Fillers on the Marine Biodegradation Behaviour of Poly(3-Hydroxybutyrate-Co-3-Hydroxyvalerate) (PHBV). *Sci. Rep.* **2021**, *11*, 911.

(16) Figueroa-Lopez, K. J.; Cabedo, L.; Lagaron, J. M.; Torres-Giner, S. Development of Electrospun Poly(3-Hydroxybutyrate-Co-3-Hydroxyvalerate) Monolayers Containing Eugenol and Their Application in Multilayer Antimicrobial Food Packaging. *Front. Nutr.* **2020**, *7*, 140.

(17) Torres-Giner, S.; Hilliou, L.; Melendez-Rodriguez, B.; Figueroa-Lopez, K. J.; Madalena, D.; Cabedo, L.; Covas, J. A.; Vicente, A. A.; Lagaron, J. M. Melt Processability, Characterization, and Antibacterial Activity of Compression-Molded Green Composite Sheets Made of Poly(3-Hydroxybutyrate-Co-3-Hydroxyvalerate) Reinforced with Coconut Fibers Impregnated with Oregano Essential Oil. *Food Packag. Shelf Life* **2018**, *17*, 39−49.

(18) Figueroa-Lopez, K. J.; Torres-Giner, S.; Angulo, I.; Pardo-Figuerez, M.; Escuin, J. M.; Bourbon, A. I.; Cabedo, L.; Nevo, Y.; Cerqueira, M. A.; Lagaron, J. M. Development of Active Barrier Multilayer Films Based on Electrospun Antimicrobial Hot-Tack Food Waste Derived Poly (3-Hydroxybutyrate- Co -3-Hydroxyvalerate) and Cellulose Nanocrystal Interlayers. *Nanomaterials* **2020**, *10*, 2356.

(19) Tomietto, P.; Loulergue, P.; Paugam, L.; Audic, J.-L. Polyhydroxyalkanoates (PHAs) for the Fabrication of Filtration Membranes. *Membrane Technology Enhancement for Environmental Protection and Sustainable Industrial Growth*; Springer Nature, 2021; pp 143−175.

(20) Li, F.; Yu, H. Y.; Li, Y.; Hussain Abdalkarim, S. Y.; Zhu, J.; Zhou, Y. "Soft-Rigid" Synergistic Reinforcement of PHBV Composites with Functionalized Cellulose Nanocrystals and Amorphous Recycled Polycarbonate. *Composites, Part B* **2021**, *206*, 108542.

(21) Paiva, A.; Matias, A. A.; Duarte, A. R. C. How Do We Drive Deep Eutectic Systems towards an Industrial Reality? *Curr. Opin. Green Sustainable Chem.* **2018**, *11*, 81−85.

(22) Basar, A. O.; Prieto, C.; Durand, E.; Villeneuve, P.; Sasmazel, H. T.; Lagaron, J. Encapsulation of β-Carotene by Emulsion Electrospraying Using Deep Eutectic Solvents. *Molecules* **2020**, *25*, 981.

(23) Paiva, A.; Craveiro, R.; Aroso, I.; Martins, M.; Reis, R. L.; Duarte, A. R. C. Natural Deep Eutectic Solvents - Solvents for the 21st Century. *ACS Sustain. Chem. Eng.* **2014**, *2*, 1063−1071.

(24) Othman, Z. S.; Hassan, N. H.; Zubairi, S. I. Alcohol Based-Deep Eutectic Solvent (DES) as an Alternative Green Additive to Increase Rotenone Yield. *AIP Conf. Proc.* **2015**, *1678*, 050004.

(25) Dai, Y.; Witkamp, G.; Verpoorte, R.; Choi, Y. H. Tailoring Properties of Natural Deep Eutectic Solvents with Water to Facilitate Their Applications. *Food Chem.* **2015**, *187*, 14−19.

(26) Roda, A.; Matias, A. A.; Paiva, A.; Duarte, A. R. C. Polymer Science and Engineering Using Deep Eutectic Solvents. *Polymers* **2019**, *11*, 912.

(27) Melendez-Rodriguez, B.; Figueroa-Lopez, K. J.; Bernardos, A.; Martínez-Máñez, R.; Cabedo, L.; Torres-Giner, S.; Lagaron, J. M. Electrospun Antimicrobial Films of Poly (3- Hydroxybutyrate- Co -3-

Hydroxyvalerate) Containing Eugenol Essential Oil Encapsulated in Mesoporous Silica Nanoparticles. *Nanomaterials* **2019**, *9*, 227.
(28) Figueroa-Lopez, K. J.; Enescu, D.; Torres-Giner, S.; Cabedo, L.; Cerqueira, M. A.; Pastrana, L.; Fuciños, P.; Lagaron, J. M. Development of Electrospun Active Films of Poly(3-Hydroxybutyrate-Co-3-Hydroxyvalerate) by the Incorporation of Cyclodextrin Inclusion Complexes Containing Oregano Essential Oil. *Food Hydrocolloids* **2020**, *108*, 106013.
(29) Pardo-Figuerez, M.; Chiva-Flor, A.; Figueroa-Lopez, K.; Prieto, C.; Lagaron, J. M. Antimicrobial Nanofiber Based Filters for High Filtration Efficiency Respirators. *Nanomaterials* **2021**, *11*, 900.
(30) Sousa, A. M. M.; Souza, H. K. S.; Uknalis, J.; Liu, S. C.; Gonçalves, M. P.; Liu, L. S. Improving Agar Electrospinnability with Choline-Based Deep Eutectic Solvents. *Int. J. Biol. Macromol.* **2015**, *80*, 139−148.
(31) Mano, F.; Aroso, I. M.; Barreiros, S.; Borges, J. P.; Reis, R. L.; Duarte, A. R. C.; Paiva, A. Production of Poly(Vinyl Alcohol) (PVA) Fibers with Encapsulated Natural Deep Eutectic Solvent (NADES) Using Electrospinning. *ACS Sustain. Chem. Eng.* **2015**, *3*, 2504−2509.
(32) Mano, F.; Martins, M.; Sá-Nogueira, I.; Barreiros, S.; Borges, J. P.; Reis, R. L.; Duarte, A. R. C.; Paiva, A. Production of Electrospun Fast-Dissolving Drug Delivery Systems with Therapeutic Eutectic Systems Encapsulated in Gelatin. *AAPS PharmSciTech* **2017**, *18*, 2579−2585.
(33) Khatri, M.; Khatri, Z.; El-Ghazali, S. E.; Hussain, N.; Qureshi, U. A.; Kobayashi, S.; Ahmed, F.; Kim, I. S. Zein Nanofibers via Deep Eutectic Solvent Electrospinning: Tunable Morphology with Super Hydrophilic Properties. *Sci. Rep.* **2020**, *10*, 15307.
(34) Fonck, E.; Feigl, G. G.; Fasel, J.; Sage, D.; Unser, M.; Rüfenacht, D. A.; Stergiopulos, N. Effect of Aging on Elastin Functionality in Human Cerebral Arteries. *Stroke* **2009**, *40*, 2552−2556.
(35) Xue, J.; Wu, T.; Dai, Y.; Xia, Y. Electrospinning and Electrospun Nanofibers: Methods, Materials, and Applications. *Chem. Rev.* **2019**, *119*, 5298−5415.
(36) Du, C.; Zhao, B.; Chen, X.; Birbilis, N.; Yang, H. Effect of Water Presence on Choline Chloride-2urea Ionic Liquid and Coating Platings from the Hydrated Ionic Liquid. *Sci. Rep.* **2016**, *6*, 29225.
(37) Angammana, C. J.; Jayaram, S. H. Analysis of the Effects of Solution Conductivity on Electrospinning Process and Fiber Morphology. *IEEE Trans. Ind. Appl.* **2011**, *47*, 1109−1117.
(38) Chen, Y.; Abdalkarim, S. Y. H.; Yu, H. Y.; Li, Y.; Xu, J.; Marek, J.; Yao, J.; Tam, K. C. Double Stimuli-Responsive Cellulose Nanocrystals Reinforced Electrospun PHBV Composites Membrane for Intelligent Drug Release. *Int. J. Biol. Macromol.* **2020**, *155*, 330−339.
(39) Vimal, S. K.; Ahamad, N.; Katti, D. S. A Simple Method for Fabrication of Electrospun Fibers with Controlled Degree of Alignment Having Potential for Nerve Regeneration Applications. *Mater. Sci. Eng., C* **2016**, *63*, 616−627.
(40) Borisova, M.; Kamalov, A.; Jayasinghe, B. M. D. N. S. Electrical and Electret Properties of Non-Woven "Spunbond" Polypropylene. *2018 IEEE 59th International Scientific Conference on Power and Electrical Engineering of Riga Technical University (RTUCON)*, 2018; pp 1−4.
(41) Borisova, M.; Kamalov, A.; Jayasinghe, N.; Chiriateva, A. Charge Relaxation and Kinetic Accumulation of Non-Woven Polypropylene and Polyimide Films. *2022 Conference of Russian Young Researchers in Electrical and Electronic Engineering (ElConRus)*; IEEE, 2022; pp 1332−1334.
(42) Bonino, C. A.; Efimenko, K.; Jeong, S. I.; Krebs, M. D.; Alsberg, E.; Khan, S. A. Three-Dimensional Electrospun Alginate Nanofiber Mats via Tailored Charge Repulsions. *Small* **2012**, *8*, 1928−1936.
(43) Cai, S.; Xu, H.; Jiang, Q.; Yang, Y. Novel 3D Electrospun Scaffolds with Fibers Oriented Randomly and Evenly in Three Dimensions to Closely Mimic the Unique Architectures of Extracellular Matrices in Soft Tissues: Fabrication and Mechanism Study. *Langmuir* **2013**, *29*, 2311−2318.
(44) Vong, M.; Speirs, E.; Klomkliang, C.; Akinwumi, I.; Nuansing, W.; Radacsi, N. Controlled Three-Dimensional Polystyrene Micro- and Nano-Structures Fabricated by Three-Dimensional Electrospinning. *RSC Adv.* **2018**, *8*, 15501−15512.
(45) Jahanbakhsh-Bonab, P.; Sardroodi, J. J.; Avestan, M. S. Electric Field Effects on the Structural and Dynamical Properties of a Glyceline Deep Eutectic Solvent. *J. Chem. Eng. Data* **2022**, *67*, 2077.
(46) Hammons, J. A.; Besford, Q. A.; Ilavsky, J.; Christofferson, A. J. Manipulating Meso-Scale Solvent Structure from Pd Nanoparticle Deposits in Deep Eutectic Solvents. *J. Chem. Phys.* **2021**, *155*, 074505.
(47) Reis, G. S. A.; de Souza, R. M. D.; Ribeiro, M. C. C. Molecular Dynamics Simulation Study of the Far-Infrared Spectrum of a Deep Eutectic Solvent. *J. Phys. Chem. B* **2022**, *126*, 5695−5705.
(48) Collins, G.; Federici, J.; Imura, Y.; Catalani, L. H. Charge Generation, Charge Transport, and Residual Charge in the Electrospinning of Polymers: A Review of Issues and Complications. *J. Appl. Phys.* **2012**, *111*, 044701.
(49) Pleşa, I.; Noţingher, P. V.; Stancu, C.; Wiesbrock, F.; Schlögl, S. Polyethylene Nanocomposites for Power Cable Insulations. *Polymers* **2019**, *11*, 24.
(50) Chen, G. Interfaces and Space Charge in Polymeric Insulating Materials. *MRS Online Proc. Libr.* **2005**, *889*, 803.
(51) Mailley, D.; Hébraud, A.; Schlatter, G. A Review on the Impact of Humidity during Electrospinning: From the Nanofiber Structure Engineering to the Applications. *Macromol. Mater. Eng.* **2021**, *306*, 2100115.
(52) Sun, B.; Long, Y. Z.; Yu, F.; Li, M. M.; Zhang, H. D.; Li, W. J.; Xu, T. X. Self-Assembly of a Three-Dimensional Fibrous Polymer Sponge by Electrospinning. *Nanoscale* **2012**, *4*, 2134−2137.
(53) Mazhar, S.; Qarni, A. A.; Haq, Y. U.; Haq, Z.; Murtaza, I.; Ahmad, N.; Jabeen, N.; Amin, S. Electrospun PVA/TiC Nanofibers for High Performance Capacitive Humidity Sensing. *Microchem. J.* **2020**, *157*, 104974.
(54) Hohman, M. M.; Shin, M.; Rutledge, G.; Brenner, M. P. Electrospinning and Electrically Forced Jets. I. Stability Theory. *Phys. Fluids* **2001**, *13*, 2201−2220.
(55) Ye, X. Y.; Jin, Y. N.; Huang, X. J.; Luo, L.; Xu, Z. K. Simulation of Electrical Field for the Formation Mechanism of Bird's Nest Patterned Structures by Electrospinning. *Chin. J. Polym. Sci.* **2013**, *31*, 514−520.
(56) Liu, L.; Dzenis, Y. A. Analysis of the Effects of the Residual Charge and Gap Size on Electrospun Nanofiber Alignment in a Gap Method. *Nanotechnology* **2008**, *19*, 355307.
(57) Gou, Y.; Liu, C.; Lei, T.; Yang, F. Nanofiber Alignment during Electrospinning: Effects of Collector Structures and Governing Parameters. *2014 International Conference on Manipulation, Manufacturing and Measurement on the Nanoscale (3M-NANO)*, 2014; pp 62−65.
(58) Li, D.; Wang, Y.; Xia, Y. Electrospinning of Polymeric and Ceramic Nanofibers as Uniaxially Aligned Arrays. *Nano Lett.* **2003**, *3*, 1167−1171.
(59) Kakoria, A.; Sinha-Ray, S. Ultrafine Nanofiber-Based High Efficiency Air Filter from Waste Cigarette Butts. *Polymer* **2022**, *255*, 125121.
(60) Leung, W. W. F.; Sun, Q. Electrostatic Charged Nanofiber Filter for Filtering Airborne Novel Coronavirus (COVID-19) and Nano-Aerosols. *Sep. Purif. Technol.* **2020**, *250*, 116886.
(61) Huiming, X.; Chen, G.; Chen, X.; Zhi, C. A Flexible Electret Membrane with Persistent Electrostatic Effect and Resistance to Harsh Environment for Energy Harvesting. *Sci. Rep.* **2017**, *7*, 8443.
(62) Zhou, T. C.; Chen, G.; Liao, R. J.; Xu, Z. Charge Trapping and Detrapping in Polymeric Materials: Trapping Parameters. *J. Appl. Phys.* **2011**, *110*, 043724.
(63) Gao, H.; He, W.; Zhao, Y. B.; Opris, D. M.; Xu, G.; Wang, J. Electret Mechanisms and Kinetics of Electrospun Nanofiber Membranes and Lifetime in Filtration Applications in Comparison with Corona-Charged Membranes. *J. Membr. Sci.* **2020**, *600*, 117879.
(64) Ullah, S.; Ullah, A.; Lee, J.; Jeong, Y.; Hashmi, M.; Zhu, C.; Joo, K. I.; Cha, H. J.; Kim, I. S. Reusability Comparison of Melt-Blown vs

https://doi.org/10.1021/acsomega.2c05838
ACS Omega 2023, 8, 3798−3811

Nanofiber Face Mask Filters for Use in the Coronavirus Pandemic. *ACS Appl. Nano Mater.* **2020**, *3*, 7231−7241.
(65) Zhou, Y.; Liu, Y.; Zhang, M.; Feng, Z.; Yu, D. G.; Wang, K. Electrospun Nanofiber Membranes for Air Filtration: A Review. *Nanomaterials* **2022**, *12*, 1077.
(66) Eichhorn, S. J.; Sampson, W. W. Statistical Geometry of Pores and Statistics of Porous Nanofibrous Assemblies. *J. R. Soc. Interface* **2005**, *2*, 309−318.
(67) Mei, Y.; Wang, Z.; Li, X. Improving Filtration Performance of Electrospun Nanofiber Mats by a Bimodal Method. *J. Appl. Polym. Sci.* **2013**, *128*, 1089−1094.
(68) Russo, F.; Castro-Muñoz, R.; Santoro, S.; Galiano, F.; Figoli, A. A Review on Electrospun Membranes for Potential Air Filtration Application. *J. Environ. Chem. Eng.* **2022**, *10*, 108452.
(69) Lv, D.; Zhu, M.; Jiang, Z.; Jiang, S.; Zhang, Q.; Xiong, R.; Huang, C. Green Electrospun Nanofibers and Their Application in Air Filtration. *Macromol. Mater. Eng.* **2018**, *303*, 1800336.

https://doi.org/10.1021/acsomega.2c05838
ACS Omega 2023, 8, 3798−3811